Longwave ($\lambda_{0.1} = 10\,\mu m$, 296 K) infrared photodetectors based on InAsSb$_{0.38}$ solid solution

© R.E. Kunkov, A.A. Klimov, N.M. Lebedeva, T.S. Lukhmyrina, B.A. Matveev, M.A. Remennyy, A.A. Usikova

Ioffe Institute, St. Petersburg, Russia

e-mail: romunkov@yandex.ru

Photodetectors based on diode heterostructure with InAsSb$_x$ photosensitive region ($x = 0.38$) with long-wave cut-off $\lambda_{0.1}$ about $10\,\mu m$ (296 K) are investigated. The dependences of dark current density and detectivity in the temperature range of $200-425$ K have been investigated. It is shown that the experimental samples are characterized by values of dark current density about $500\,A/cm^2$ at room temperature, detectivity $1.2 \cdot 10^9$ and $5 \cdot 10^9\,cmHz^{1/2}W^{-1}$ at room temperature and 250 K, respectively, and diffusion mechanism of current flow in the temperature range $200-350$ K.

Introduction

Infrared radiation receivers operating in the long-wave region of the spectrum $(8-14\,\mu m)$ are key components of both thermal imaging and heat direction finding systems, and gas analytical equipment in life safety systems and medical equipment. Photodetectors based on diode heterostructures with an active layer of InAs$_{1-x}$Sb$_x$ solid solutions are a promising alternative to both the most common photodetectors based on Cadmium–Mercury–Tellurium (CMT) [1,2] semiconductors and photodetectors made from A^{III}B^V semiconductors based on superlattices [3,4]. Depending on the composition of the photosensitive layer, InAsSb photodetectors can operate both in the mid-wave $(3-5\,\mu m)$ [5] and long-wave $(8-14\,\mu m)$ infrared regions of the spectrum [6].

Experimental results

Epitaxial structures N-InAsSb/InAsSb/P-InAsSbP were obtained on substrates of undoped n^0-InAs oriented in the (100) plane by liquid-phase epitaxy LPE and contained a buffer gradient layer of N-InAsSb with a thickness of $2.5-3.0\,\mu m$, photosensitive region InAsSb$_{0.38}$ with a thickness of $3.0-3.2\,\mu$ m and a contact layer P-InAsSbP with a thickness of $1.5-2\,\mu m$, doped with Zn to a concentration of $p \geq 5 \cdot 10^{17}\,cm^{-3}$. This work presents the results for a heterostructure with number № 2052. Experimental samples of photodetector chips were obtained using multistage chemical photolithography methods. Samples of the „flip-chip" design had a square shape with a size of $250 \times 250\,\mu m$ and a round mesa with a diameter of $100\,\mu m$, limiting the area of the photosensitive region. To obtain experimental samples of photodetectors, immersion joining of the resulting chips

with lenses made of germanium with an antireflective coating with a diameter of 3.5 mm was carried out.

Figure 1 shows the current-voltage characteristics (a) and dark current densities (b) in the temperature range $200-425$ K for a heterostructure sample with number № 2052. Besides, Fig. 1, b shows the results for a sample from a heterostructure with the number № 1511z from the work [7] (2021) for the development and research of photodetectors with a similar composition of the photosensitive region.

As can be seen from the figure, the heterostructures obtained in this work are characterized by lower dark current densities at room temperature and a less sharp temperature dependence compared to previous results obtained in [7]. In addition to this, the temperature dependence of the dark current density is well approximated in the temperature range $200-350$ K using the following relation:

$$J_0(T) \propto e^{\left(\frac{-h\nu_{0.1}}{kT}\right)}, \qquad (1)$$

which indicates the dominance of the diffusion mechanism of current flow. In this formula $h\nu_{0.1}$ —- is the energy of the long-wave limit of photosensitivity at a level of 0.1 from the maximum, the value of which is close to the band gap of the photosensitive region (E_g).

With a further decrease in temperature, a transition to the tunnel mechanism of current flow is most likely, which can be evidenced by approximation using the relation

$$J_0(T) \propto e^{\left(\frac{-h\nu_{0.1}}{4kT}\right)}. \qquad (2)$$

However, this temperature range is beyond the scope of the study.

Figure 2 shows the spectra of detection detectivity (a) and values $h\nu_{max}$, $h\nu_{0.5}$ and $h\nu_{0.1}$ (b) in the temperature range $200-425$ K. As can be seen from the figure, the
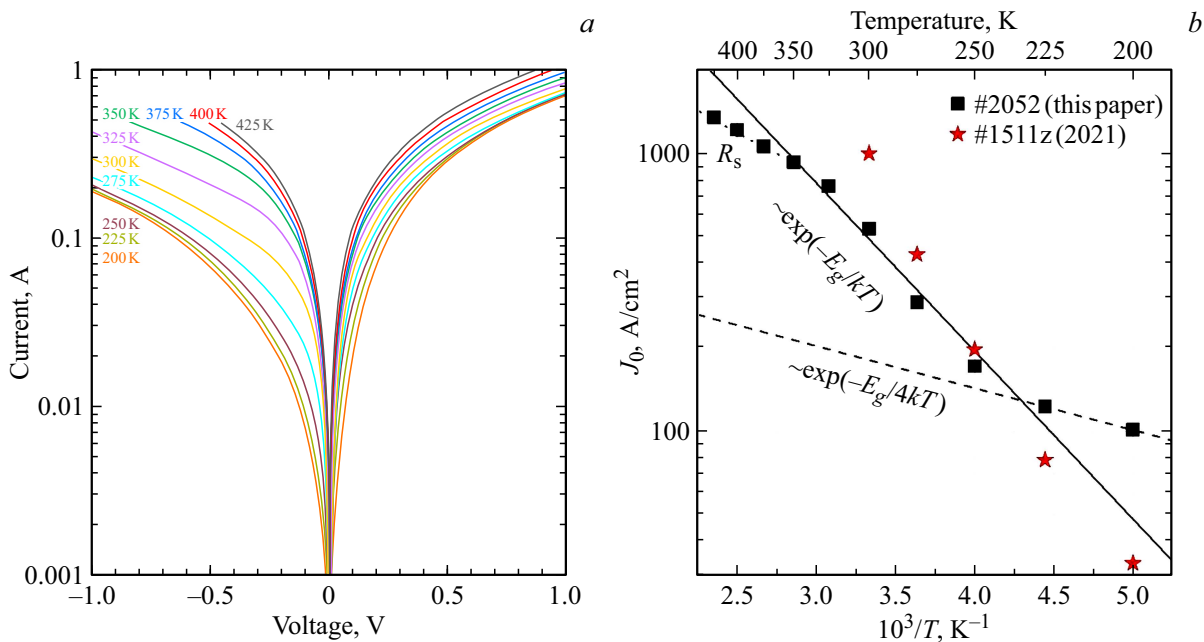
Figure 1. Current-voltage dependences in the temperature range $200-425$ K (*a*) and the dependence of the dark current density on temperature (*b*).
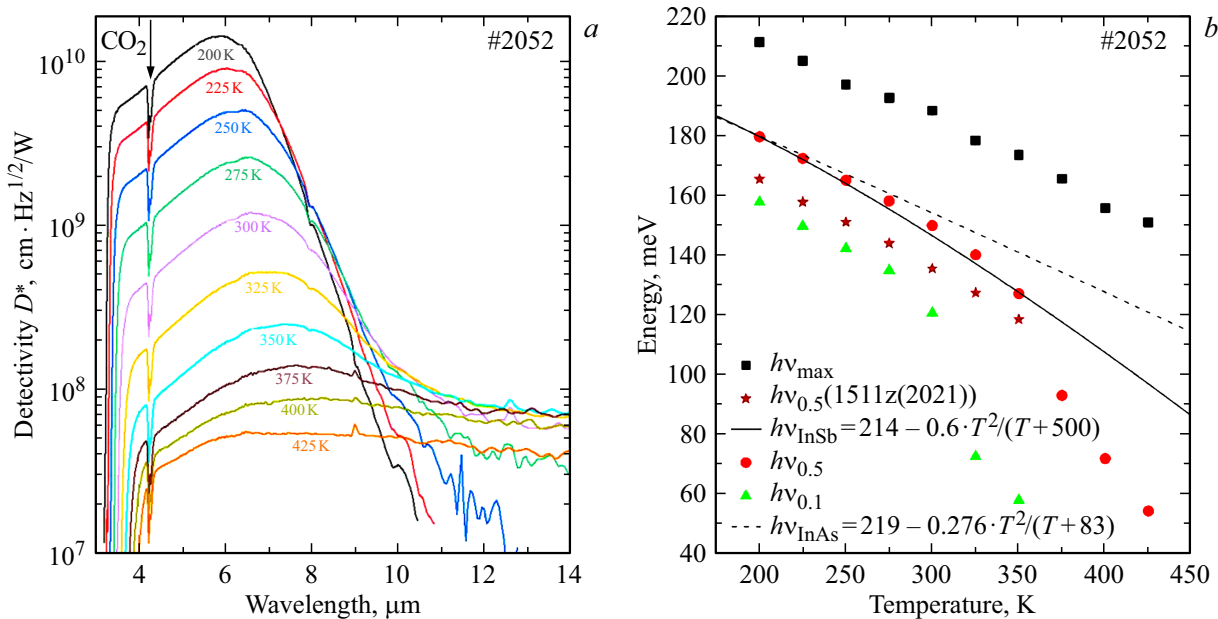
Figure 2. Spectral dependence of detectivity in the temperature range $200-425$ K (*a*) and temperature dependence of energy $h\nu$ of the long-wave limit of photosensitivity at levels 0.5 and 0.1 from the maximum (*b*).

experimental samples are characterized by detection detectivity values of approximately $1.2 \cdot 10^9 \, \text{cmHz}^{1/2}\text{W}^{-1}$ at room temperature and $5 \cdot 10^9 \, \text{cmHz}^{1/2}\text{W}^{-1}$ at 250 K, achievable with the help of thermoelectric cooling.

When the temperature rises over $325-350$ K, there is behavior of the long-wavelength boundary, which differs from that of both shorter-wavelength photodiodes and photodetectors with similar compositions described earlier [7]. This difference is most clearly illustrated by the temperature

dependence of energy at the level of 0.5 and 0.1 on the maximum photosensitivity (Fig. 2, *b*). The figure shows a significant deviation of the experimental data at elevated temperatures from the approximation, taking into account the dependence of the InSb band gap on temperature [8].

Figure 3 shows a comparison of the results of this work with the dependences of the band gap on composition and the dependences of dark current densities on the long-wavelength limit of photosensitivity, taken from literature
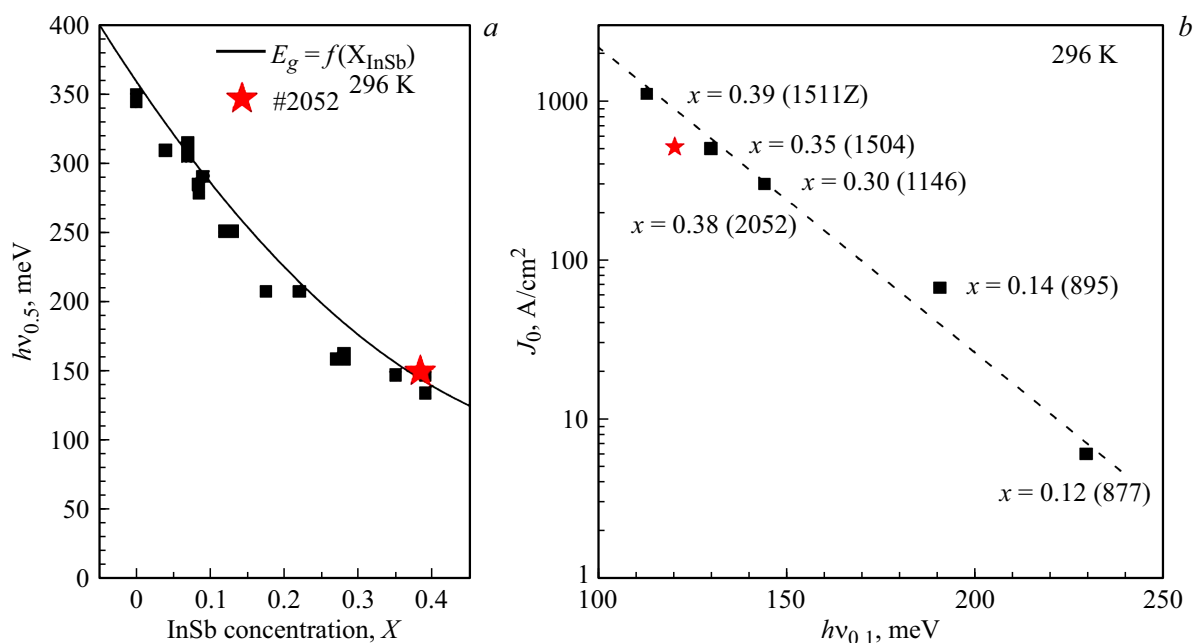
Figure 3. The dependence of the band gap on the composition (a) and the dependence of the dark current density on the long-wave boundary $h\nu_{0.1}$ (b) at 296 K in comparison with data from the literature: asterisks — this work , squares — previous work, including [7], solid curve (a) and dashed line (b) — approximations of experimental data.

sources, including from our previous works [5–7]. The obtained values of the band gap at room temperature are consistent with the results of previous studies; however, in the present work, there is a decrease in the dark current density of up to 2 times [7] One of the likely reasons for the decrease in current density is an improvement in the crystallographic quality of the resulting layers, in particular, a decrease in the number of mismatch dislocations and their concentration at the interface between the substrate and the wide-band „buffer" layer, which leads to a decrease in their influence on the optical and electrical characteristics of photodetectors based on such structures. This assumption is based on the study of the resulting epitaxial structures using transmission electron microscopy, the results of which will be discussed in a special publication.

Conclusion

Experimental samples of long-wavelength photodetectors with an active region from the InAsSb$_x$ ($x \approx 0.38$) solid solution with a long-wavelength photosensitivity limit $\lambda_{0.1}$ of approximately $10\,\mu$m (300 K) were obtained and their photoelectric properties were studied in the temperature range $200-425$ K. In comparison with the results of previous work, a decrease in the density of dark currents by a factor of two and an increase in the detection detectivity by one and a half times at room temperature to values of 500Å/cm^2 and $1.2 \cdot 10^9$ cmHz$^{1/2}$W^{-1}, respectively, were demonstrated. At a temperature of 250 K, the value of detection detectivity $5 \cdot 10^9$ cmHz$^{1/2}$W^{-1} was obtained, which

allows the use of these photodetectors for thermoelectric cooling.

Conflict of interest

The authors declare that they have no conflict of interest.

References

[1] A. Rogalski. Infrared Phys. Technol., **54** (3), 136 (2011). DOI: 10.1016/j.infrared.2010.12.003
[2] A. Rogalski, P. Martyniuk, M. Kopytko, W. Hu. Appl. Sci., **11** (2), 501 (2021). DOI: 10.3390/s23177564
[3] D.H. Wu, A. Dehzangi, Y.Y. Zhang, M. Razeghi. Appl. Phys. Lett., **112** (24), 241103 (2018). DOI: 10.1063/1.5035308
[4] A. Rogalsky, M. Kopytko, P. Martyniuk. *Antimonide-based infrared detectors* (SPIE press, Bellingham, 2018).
[5] N.D. Il'inskaya, S.A. Karandashev, A.A. Lavrov, B.A. Matveev, M.A. Remennyi, N.M. Stus', A.A. Usikova. Infrared Phys. Technol., **88**, 223 (2018).
[6] R.E. Kunkov, A.A. Klimov, N.M. Lebedeva, T.C. Lukhmyrina, B.A. Matveev, M.A. Remennyy. J. Phys.: Conf. Ser., **1695** (1), 012077 (2020).
[7] A.A. Klimov, R.E. Kunkov, A.A. Lavrov, N.M. Lebedeva, T.C. Lukhmyrina, B.A. Matveev, M.A. Remennyi. J. Phys.: Conf. Ser., **1851** (1), 012019 (2021).
[8] *New Semiconductor Materials. Biology systems. Characteristics and Properties* [Electronic resource]. URL: http://www.matprop.ru/InSb_bandstr

Translated by E.Potapova